Supplementary Information

A novel Co-based MOF/Pd composite: synergy of charge-transfer towards the electrocatalytic oxygen evolution reaction

Luis A. Alfonso-Herrera[a], Leticia M. Torres-Martínez[a,b] and J.Manuel Mora-Hernandez[c,*]

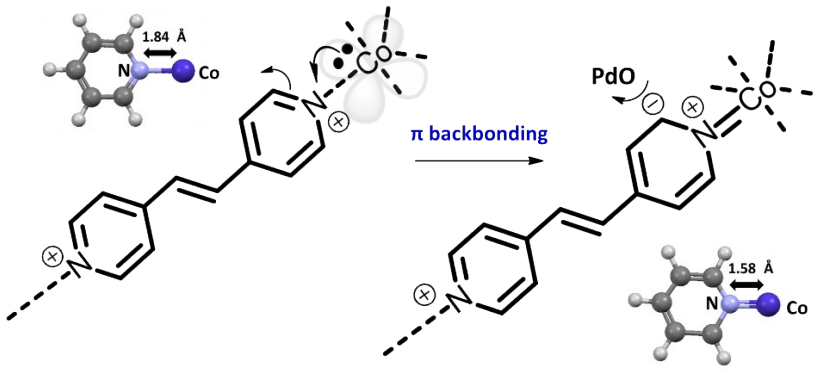

Fig. S1 - Resonance structures and double bond stabilization produced by a retro-donation effect

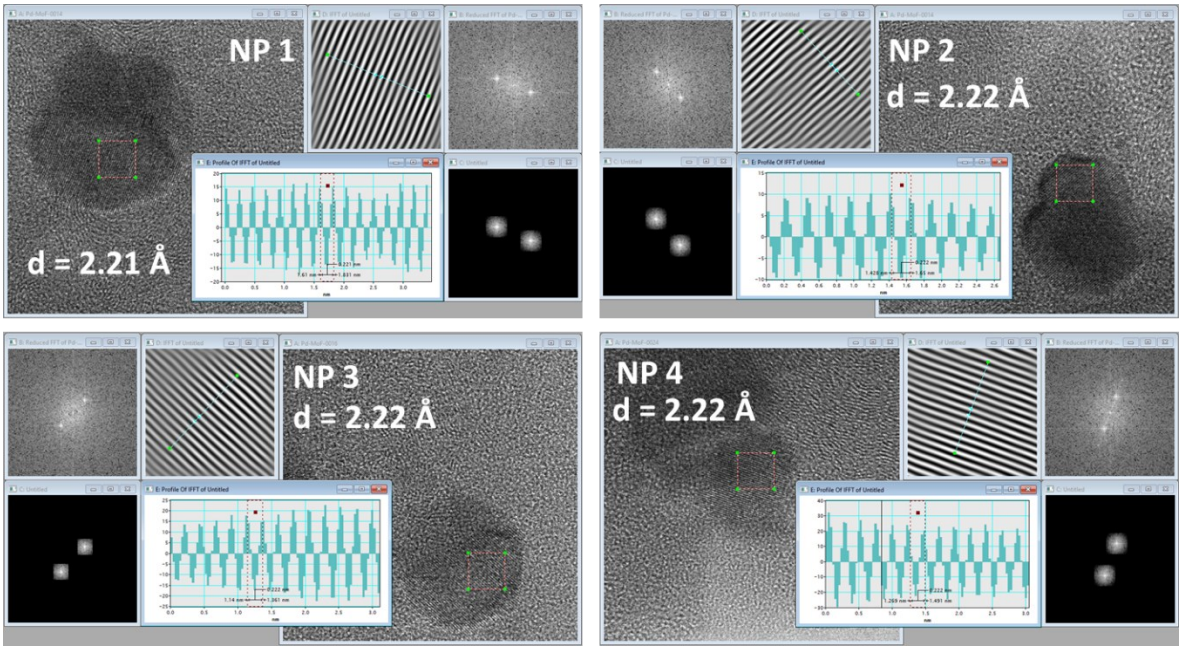

Fig. S2 – Measurement of the interplanar distance for the LEEL-037/Pd-C composite

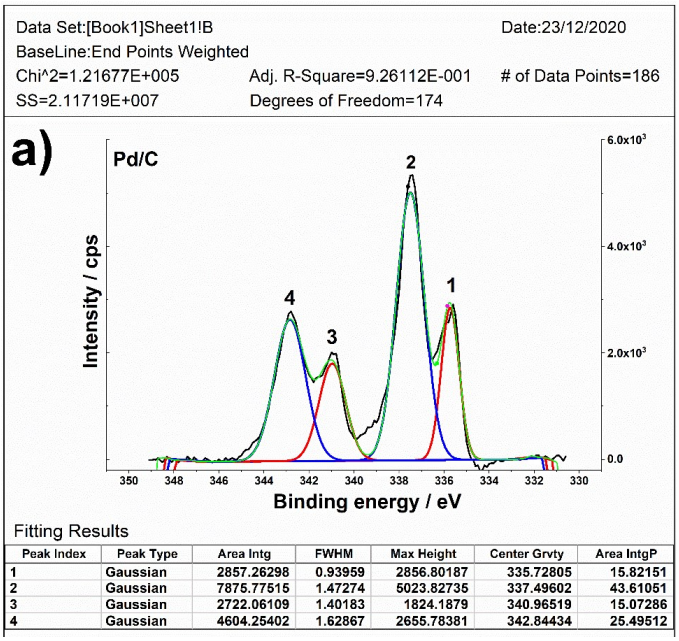

Fitting Results

Peak Index	Peak Type	Area Intg	FWHM	Max Height	Center Grvty	Area IntgP
1	Gaussian	2857.26298	0.93959	2856.80187	335.72805	15.82151
2	Gaussian	7875.77515	1.47274	5023.82735	337.49602	43.61051
3	Gaussian	2722.06109	1.40183	1824.1879	340.96519	15.07286
4	Gaussian	4604.25402	1.62867	2655.78381	342.84434	25.49512

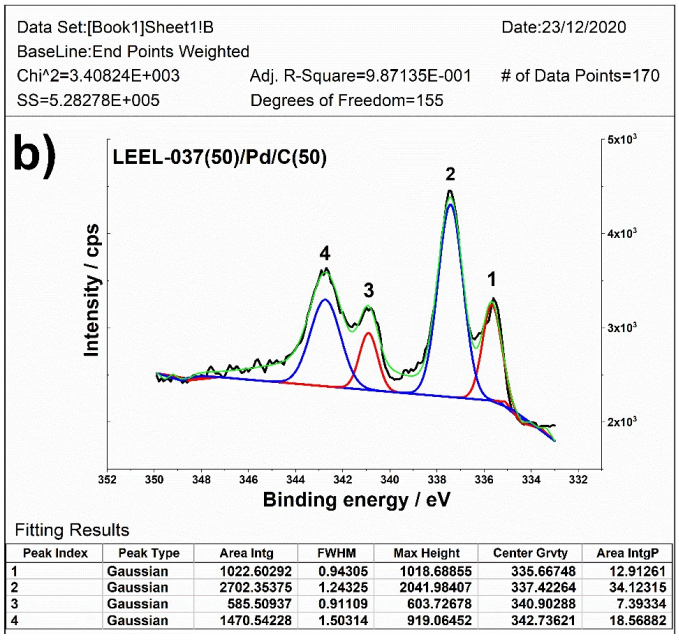

Fitting Results

Peak Index	Peak Type	Area Intg	FWHM	Max Height	Center Grvty	Area IntgP
1	Gaussian	1022.60292	0.94305	1018.68855	335.66748	12.91261
2	Gaussian	2702.35375	1.24325	2041.98407	337.42264	34.12315
3	Gaussian	585.50937	0.91109	603.72678	340.90288	7.39334
4	Gaussian	1470.54228	1.50314	919.06452	342.73621	18.56882

Fig. S3 – Peaks analysis to determine the Pd and PdO percentage in a) Pd/C and b) LEEL-037(50)/Pd/C(50) electrocatalysts

Electrochemical surface area calculation

To calculate the ECSA, it is necessary to determine the coulombic charge (*Q*) corresponding to the oxide reduction peak area from the current vs. potential (*I vs. E*) CV plot. The following images for Pd/C (left) and LEEL-037(50)/Pd-C(50) (right) are depicted as an example to show the calculation:

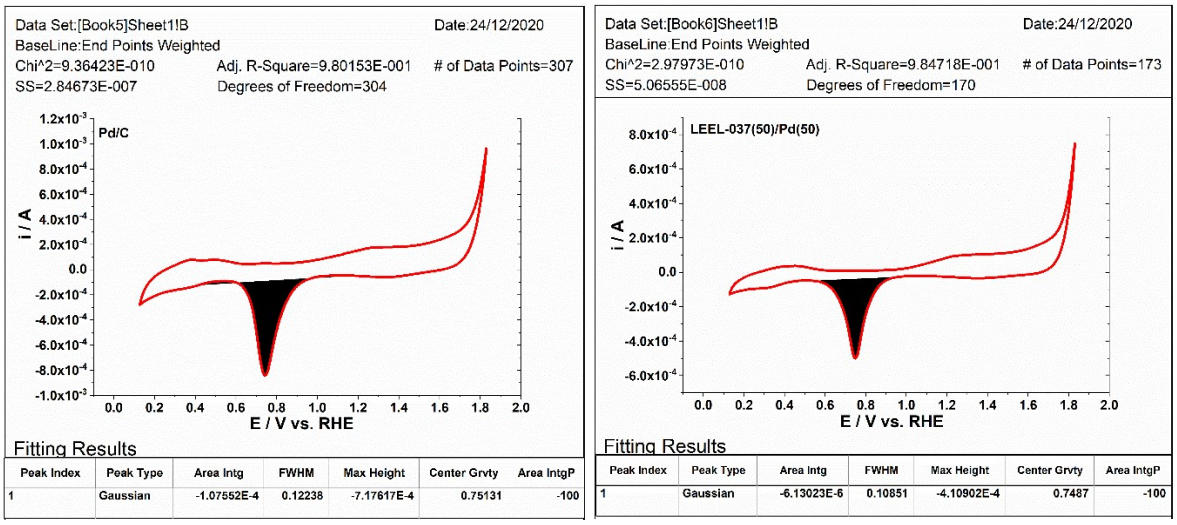

Fig. S4 – Coulombic charge determination for Pd/C (left) and LEEL-037(50)/Pd-C(50) (right)

The coulombic charge for Pd/C and LEEL-037(50)/Pd-C(50) electrocatalyst are 107.55 µA*V and 61.30 µA*V, respectively. The ECSA is defined as follows:

$$\text{ECSA} = \frac{Q}{Q_{PdO} * Pd_m * v} \qquad (1)$$

where Q is the PdO coulombic charge (µA*V), Q_{PdO} is the charge required for the reduction of PdO monolayer, which is assumed as 420 µC cm^{-2} [1,2] Pd_m is the Pd loading in "mg", and v is the scan rate in V s^{-1} (0.05 V s^{-1} for this experimentation). The mass percentage (wt.%) of bare Pd/C and LEEL-037/Pd-C electrodes is described in Table S1.

Table S1. Electrocatalysts composition

Electrocatalyst	Vulcan Carbon XC-72 (wt.%)	Vulcan Carbon XC-72 (mg)	Pd (wt.%)	Pd (mg)	LEEL-037 (wt.%)	LEEL-037 (mg)
Pd/C	70	7	30	3	0	0
LEEL-037(25)/Pd-C(75)	52.5	5.25	22.5	2.25	25	2.5
LEEL-037(50)/Pd-C(50)	35	3.5	15	1.5	50	5
LEEL-037(75)/Pd-C(25)	15	1.5	7.5	.75	75	7.5

To calculate the Pd loading for Pd/C and LEEL-037(50)/Pd-C(50), we know that we used 3 µL of the electrocatalytic ink containing 10 mg of the electrocatalyst in turn, 1250 µL of water, and 250 µL of 5 wt.% Nafion® solution (density ≈ 1 mg ml^{-1}). The Pd loading (Pd_m) was calculated as follows:

For Pd/C electrocatalyst;

$$\text{Pd}_m = \frac{10\ mg\ Pd/C}{1.5\ ml\ (water - Nafion)} * 0.003 \text{ ml (ink aliquot)} * 0.3 \text{ wt.\% Pd} = 0.006 \text{ mg Pd}$$

For LEEL-037(50)/Pd-C(50) electrocatalyst;

$$Pd_m = \frac{10\ mg\ LEEL-037(50)Pd/C(50)}{1.5\ ml\ (water-Nafion)} * 0.003\ ml\ (ink\ aliquot) * 0.15\ wt.\%\ Pd = 0.003\ mg\ Pd$$

Substituting the data in eq.1, the ECSAs for Pd/C and LEEL-037(50)/Pd-C(50) electrocatalyst are 85.36 $m^2\ g_{Pd}^{-1}$ and 97.3 $m^2\ g_{Pd}^{-1}$, respectively.

Table S2. Comparison of physicochemical and electrocatalytic properties for Ru and Ir free electrocatalysts used to carry out the OER in alkaline medium.

Material	Operational overpotential at 10 mA/ cm^2 (mV)	Tafel slope (mV dec^{-1})	Crystal size (nm)	Electrolyte	Reference
LEEL-037(25)/Pd-C(75)	430	173	30.80*	KOH 0.5 M	This work
LEEL-037	480	104	35.80	KOH 0.5 M	This work
Ni-Co@carbon	243	67	---	KOH 1.0 M	[3]
Co_3O_4/NC	325	80	---	KOH 1.0 M	[4]
Ni-BDC	360	57	45.03	KOH 1.0 M	[5]
$Ni_{0.75}Fe_{0.25}$BDC	310	43.7	17.11	KOH 0.1 M	[6]
Fe@BIF-91	350	71	63.72	KOH 1.0 M	[7]
ZIF-67/CoNiAl-LDH/NF	303	88	46.23	KOH 1.0 M	[8]
FeNi@CNF	356	62.6	21.89	KOH 1.0 M	[9]
β-Ni(OH)2/Cu_2S hybrid nanosheets	500	89	29.1	KOH 0.1 M	[10]
NiTe	388	117	27.98	KOH 1.0 M	[11]
Co_3O_4	394	149.6	14.36	KOH 1.0 M	[12]
Fe_2P@NPC	510	140	-----	KOH 1.0 M	[13]
NiFeP@PC	460	131	25.68		
Ni_2P@NPC	440	110	13		
$Ni_{1.5}Fe_{0.5}P$@NPC	410	87	26.9		
CoP@NG	354	63.8	17.95	KOH 1.0 M	[14]
ZnO@NMC nanocomposite	570	318	41.75	KOH 0.5 M	[15]

*Crystallite size calculated at the main diffraction peak (2θ) for Pd/C (40.3°).

Table S3. Calculated values of the equivalent circuit elements for the samples

Sample	Rs (Ω)	CPE-T	CPE-P	Rct (Ω)	x^2
Pd/C	32.22	$3.8X10^{-4}$	0.8176	80.13	$2.5X10^{-3}$
MOF	32.85	$1.8X10^{-4}$	0.6886	64.20	$1.9X10^{-3}$
LEEL-037(25)/Pd-C(75)	33.80	$9\ X10^{-5}$	0.7558	36.42	$2.6X10^{-3}$
LEEL-037(50)/Pd-C(50)	33.70	$6.9\ X10^{-4}$	0.6909	52.02	$1.7X10^{-3}$
LEEL-037(75)/Pd-C(25)	33.23	$2.2\ X10^{-4}$	0.6968	64.27	$2.2X10^{-3}$

References

[1] A.N. Correia, L.H. Mascaro, S.A.S. Machado, L.A. Avaca, Active surface area determination of Pd-Si alloys by H-adsorption, Electrochim. Acta. (1997). https://doi.org/10.1016/S0013-4686(96)00232-0.

[2] D.A.J. Rand, R. Woods, The nature of adsorbed oxygen on rhodium, palladium and gold electrodes, J. Electroanal. Chem. (1971). https://doi.org/10.1016/S0022-0728(71)80039-6.

[3] G. Wu, S. Liu, G. Cheng, H. Li, Y. Liu, Ni-Co@carbon nanosheet derived from nickelocene doped Co-BDC for efficient oxygen evolution reaction, Appl. Surf. Sci. 545 (2021) 148975. https://doi.org/10.1016/j.apsusc.2021.148975.

[4] H. Li, M. Tan, C. Huang, W. Luo, S.F. Yin, W. Yang, Co2(OH)3Cl and MOF mediated synthesis of porous Co3O4/NC nanosheets for efficient OER catalysis, Appl. Surf. Sci. 542 (2021) 148739. https://doi.org/10.1016/j.apsusc.2020.148739.

[5] D. Zhu, J. Liu, L. Wang, Y. Du, Y. Zheng, K. Davey, S.Z. Qiao, A 2D metal-organic framework/Ni(OH) 2 heterostructure for an enhanced oxygen evolution reaction, Nanoscale. 11 (2019) 3599–3605. https://doi.org/10.1039/c8nr09680e.

[6] Y. Hao, Q. Liu, Y. Zhou, Z. Yuan, Y. Fan, Z. Ke, C. Su, G. Li, A 2D NiFe Bimetallic Metal–Organic Frameworks for Efficient Oxygen Evolution Electrocatalysis, ENERGY Environ. Mater. (2019). https://doi.org/10.1002/eem2.12024.

[7] T. Wen, Y. Zheng, J. Zhang, K. Davey, S.Z. Qiao, Co (II) Boron Imidazolate Framework with Rigid Auxiliary Linkers for Stable Electrocatalytic Oxygen Evolution Reaction, Adv. Sci. (2019). https://doi.org/10.1002/advs.201801920.

[8] J. Xu, Y. Zhao, M. Li, G. Fan, L. Yang, F. Li, A strong coupled 2D metal-organic framework and ternary layered double hydroxide hierarchical nanocomposite as an excellent electrocatalyst for the oxygen evolution reaction, Electrochim. Acta. (2019). https://doi.org/10.1016/j.electacta.2019.03.210.

[9] Y. Li, M. Lu, P. He, Y. Wu, J. Wang, D. Chen, H. Xu, J. Gao, J. Yao, Bimetallic Metal-Organic Framework-Derived Nanosheet-Assembled Nanoflower Electrocatalysts for Efficient Oxygen Evolution Reaction, Chem. - An Asian J. (2019). https://doi.org/10.1002/asia.201900328.

[10] D. Yang, L. Gao, J.H. Yang, Facile synthesis of ultrathin Ni(OH)2-Cu2S hexagonal nanosheets hybrid for oxygen evolution reaction, J. Power Sources. (2017). https://doi.org/10.1016/j.jpowsour.2017.05.034.

[11] L. Zhong, Y. Bao, X. Yu, L. Feng, An Fe-doped NiTe bulk crystal as a robust catalyst for the electrochemical oxygen evolution reaction, Chem. Commun. (2019). https://doi.org/10.1039/c9cc04429a.

[12] Z. Liu, Z. Xiao, G. Luo, R. Chen, C.L. Dong, X. Chen, J. Cen, H. Yang, Y. Wang, D. Su, Y. Li, S. Wang, Defects-Induced In-Plane Heterophase in Cobalt Oxide Nanosheets for Oxygen Evolution Reaction, Small. (2019). https://doi.org/10.1002/smll.201904903.

[13] J. Wang, F. Ciucci, In-situ synthesis of bimetallic phosphide with carbon tubes as an active electrocatalyst for oxygen evolution reaction, Appl. Catal. B Environ. (2019). https://doi.org/10.1016/j.apcatb.2019.05.009.

[14] Y. Lu, W. Hou, D. Yang, Y. Chen, CoP nanosheets in-situ grown on N-doped graphene as an efficient and stable bifunctional electrocatalyst for hydrogen and oxygen evolution reactions, Electrochim. Acta. (2019). https://doi.org/10.1016/j.electacta.2019.03.208.

[15] M. Ubaidullah, A.M. Al-Enizi, S. Shaikh, M.A. Ghanem, R.S. Mane, Waste PET plastic derived ZnO@NMC nanocomposite via MOF-5 construction for hydrogen and oxygen evolution reactions, J. King Saud Univ. - Sci. (2020). https://doi.org/10.1016/j.jksus.2020.03.025.